Journal of Physiology (1990), **429**, *pp.* 47–62
With 10 *figures*
Printed in Great Britain

ELECTRICAL RESISTANCE ACROSS THE BLOOD–BRAIN BARRIER IN ANAESTHETIZED RATS: A DEVELOPMENTAL STUDY

BY ARTHUR M. BUTT, HAZEL C. JONES* AND N. JOAN ABBOTT

From the Physiology Group, Biomedical Sciences Division, King's College London, Campden Hill Road, London W8 7AH

(*Received 22 March 1990*)

SUMMARY

1. Ion permeability of the blood–brain barrier was studied by *in situ* measurement of transendothelial electrical resistance in anaesthetized rats aged between 17 days gestation and 33 days after birth, and by electron microscopic examination of lanthanum permeability in fetal and neonatal rats aged up to 10 days old.

2. The blood–brain barrier in 17- to 20-day fetuses had a resistance of 310 Ω cm^2 but was impermeable to lanthanum, and therefore had properties intermediate between leaky and tight epithelia.

3. From 21 days gestation, the resistance was 1128 Ω cm^2, indicating a tight blood–brain barrier and low ion permeability. There was little further change in barrier resistance after birth, and in 28- to 33-day rats, when the brain barrier systems are mature in other ways, vessels had a mean resistance of 1462 Ω cm^2.

4. In the tight blood–brain barrier, arterial vessels had a significantly higher resistance than venous vessels, 1490 and 918 Ω cm^2 respectively. In vessels less than 50 μm diameter and within the normal 60 min experimental period, there was no significant variation in vessel resistance.

5. Hyperosmotic shock caused a rapid decay in resistance (maximal within 5 min), and after disruption of the blood–brain barrier, vessel resistance was 100–300 Ω cm^2 in both arterial and venous vessels, and the effect was reversible. After the application of metabolic poisons (NaCN plus iodoacetate) and low temperature there was a similarly low electrical resistance.

6. It is concluded that the increase in electrical resistance at birth indicates a decrease in paracellular ion permeability at the blood–brain barrier and is required for effective brain interstitial fluid ion regulation.

INTRODUCTION

In adult mammals, brain interstitial fluid ions are maintained independently of changes in plasma concentrations by the blood–brain barrier (Bradbury, 1979). Ion regulation by the blood–brain barrier is determined by its low permeability and by transport processes at the cerebral endothelium (e.g. Smith & Rapoport, 1986). The permeability barrier is sited at the tight intercellular junctions between cerebral

* Address for correspondence and reprint requests: Dr H. C. Jones, Physiology, Biomedical Sciences Division, King's College London, Campden Hill Road, Kensington, London W8 7AH.

MS 8370

endothelial cells as determined by electron microscopy (Brightman & Reese, 1969), and these junctions are impermeable to ionic lanthanum (Bouldin & Krigman, 1975). During development in the rat, the ability to maintain interstitial potassium and calcium during acute changes in plasma concentrations was not present in fetuses, but became evident at birth (Jones & Keep, 1987, 1988). This onset of ion homeostasis could be due to a change in permeability at the blood–brain barrier or it could be due to the activation of cellular ion transport mechanisms. In the frog, brain surface vessels have characteristic properties of the blood–brain barrier, that is, they are impermeable to ionic lanthanum (Bundgaard, 1982), have a high electrical resistance and therefore low paracellular ion permeability (Crone & Olesen, 1982; Crone, 1984; Olesen, 1989), and possess ion transport mechanisms (Abbott, Butt & Wallis, 1986). We have studied blood–brain barrier ion permeability during development in the rat, by measuring the transendothelial electrical resistance and by an electron microscopic examination of lanthanum permeability in brain surface vessels. These experiments show that there is an increase in electrical resistance and therefore a decrease in ion permeability which coincides with the onset of ion regulation at birth. However, interendothelial junctions which were tight to lanthanum were present even in fetuses.

A preliminary report of some of this work has been presented to the Physiological Society (Butt & Jones, 1990).

METHODS

Animals

Rats (CFY strain) were used at 17–21 days gestation and 1–33 days after birth. Rats were anaesthetized with intraperitoneal injections of pentobarbitone (30–60 mg/kg), and maintained at 37 °C on a warm water-filled Perspex bath. For pregnant rats, mothers were anaesthetized and a tracheotomy was performed, and then a fetus exteriorized as detailed previously (Jones & Keep, 1987). The skin above the cranium was removed and a plastic ring fixed to the skull with cyanoacrylate glue. The head was viewed through a binocular microscope (Kyowa) and illuminated with a fibre optic (cold) light source. A piece of parietal bone of about 2–5 mm^2, depending on age, was removed directly with a scalpel, except in 28- to 33-day rats where the skull was initially thinned with a dental drill. The dura and arachnoid maters were carefully removed to expose the pial surface of the cerebrum. Throughout the operation and the experiment the chamber was continuously perfused with filter-sterilized (Millipore, 0·22 μm pore size) artificial cerebrospinal fluid (CSF), containing (in mM): NaCl, 138; $NaHCO_3$, 4·2; KCl, 3; $MgSO_4$, 1·2; $CaCl_2$, 1·26; HEPES, 10; at pH 7·4 and 280 mosM. The superfusate temperature was kept constant at 35 °C throughout the experiment, but variations between 32 and 37 °C did not affect the results.

Arterial and venous vessels of 10–60 μm diameter were systematically studied at all ages. Venous vessels were recognized as dark red, with blood flowing out from the interior of the brain and had many converging branches. Arterial vessels were a brighter red, with blood flowing towards the brain interior and had fewer branches.

Electrical measurement

The technique of Crone & Olesen (1982) was used for measurement of transendothelial electrical resistance. The method is based on the infinite leaky cable theory developed by Hodgkin (1951) and Katz (1966). In brief, current injected through a microelectrode tip inside a blood vessel causes a voltage displacement which decays exponentially with distance from the current source. The fall in voltage is due in part to leakage of current across the vessel wall which is defined by the length constant (Katz, 1966) of the vessel and is a function of its ionic permeability. Transendothelial resistance (R_m) is dependent on the internal resistance of the vessel (r_i), the length constant (λ) and the area of wall, according to the equation (Crone & Olesen, 1982):

$$R_m = r_i \lambda^2 2\pi a, \quad (1)$$

where a is the radius of the vessel and r_i is determined by the resistivity of blood (ρ_i) and the vessel cross-sectional area ($r_i = \rho_i/\pi a^2$).

Vessel radius was measured using an eye-piece graticule with 20 μm divisions at $\times 90$ magnification. The resistivity of rat blood was taken as 90 Ω cm, estimated from the resistivity of

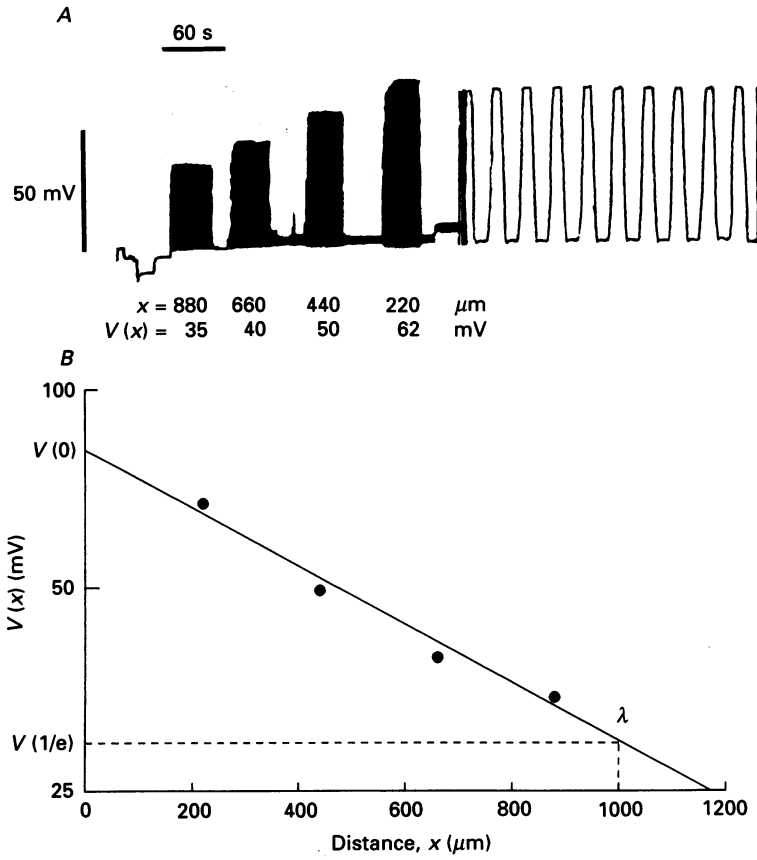

Fig. 1. *A*, measurement of microvessel length constant (λ). Record of microvessel which was impaled with two microelectrodes during current injection into the lumen through one microelectrode. The voltage deflection was measured through the second microelectrode at four decreasing distances in each vessel. The fall in voltage with increasing distance between the electrodes is due to the leak of current through the vessel wall. The trace illustrates a typical record in which the voltage displacement clearly increased as the electrodes were brought closer. *B*, voltage was plotted as a log against distance between the current-injecting and voltage-measuring electrodes. The plots are taken from the results in *A*. A line was drawn by linear regression to give $V(0)$, the voltage at zero distance, and λ, the length constant, which is defined as the distance at which V fell to 1/e.

saline (154 mM-NaCl = 62 Ω cm) and allowing for a haematocrit of 40%. The haematocrit was measured in a few rats and was not found to vary with age.

Blood vessels were impaled individually with two 3 M-KCl-filled microelectrodes, one to pass current and a second to measure the voltage; the preparation was earthed via a 3 M-KCl–agar bridge. Voltage pulses were delivered at 2·5 Hz with a stimulus duration of 200 ms (Farnell Physiological Stimulator and Stimulus Isolator Unit), converted at the amplifier (WPI duo 773 electrometer) to constant current pulses of 50–100 nA, and passed through a microelectrode (2–5 MΩ) into the vessel lumen. The voltage deflection was measured with the second

microelectrode (5–10 MΩ) connected to a high input impedance amplifier (WPI duo 773). For each vessel, voltage was measured at three to four decreasing distances between the two electrodes, as determined by the eye-piece graticule (Fig. 1*A*). The results were taken directly from pen recordings and log voltage was plotted against distance (Fig. 1*B*). The length constant, λ, is defined

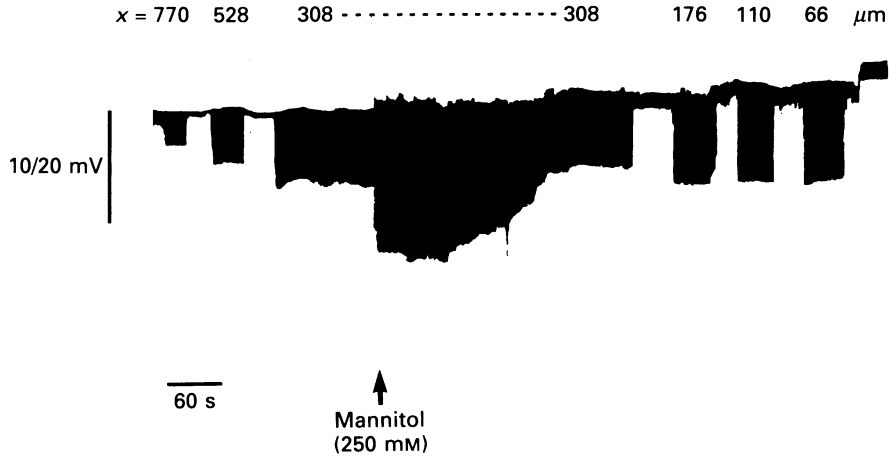

Fig. 2. Effect of hyperosmotic shock on transendothelial electrical resistance. The trace illustrates a typical continuous record of the decay in voltage displacement during addition of 250 mM-mannitol to the normal superfusate (final osmolarity = 530 mosM). The vessel was impaled with two microelectrodes, current was injected through one into the vessel lumen, and the voltage deflection measured with the second electrode at three decreasing distances. At the third distance, the voltage deflection was measured during the turnover from CSF to mannitol, to provide a continuous record of barrier disruption; note that the scale was altered at the time of mannitol application (arrow), so that the bar represents 20 mV before and 10 mV during mannitol. The voltage deflection was then measured at a further three decreasing distances in the same vessel, to provide the resistance before and during hyperosmotic disruption.

as the distance at which the voltage falls to 1/e (Katz, 1966; Crone & Olesen, 1982; Olesen & Crone, 1983). Lines were drawn by linear regression and $V(0)$, the voltage at zero distance, and $V(1/e)$ were calculated by extrapolation to give λ for each vessel. Vessels with low linear correlation coefficients ($r < 0{\cdot}90$) were discarded.

Blood–brain barrier disruption

The effect of hyperosmotic shock was determined in 7- to 10-day-old rats, by addition of 250 mM-mannitol to the superfusate, to give a final osmolarity of 530 mosM. In each rat ($n = 5$), control resistance was measured in four to five vessels in normal superfusate, then in another four to five vessels during mannitol exposure (5–15 min), and finally in a further four to five vessels in normal CSF during a recovery period of 5–15 min. Superfusate solutions were changed rapidly using a multitap system (Omnifit, Cambridge). In each rat, the voltage deflection was measured in one vessel during the turnover from CSF to mannitol, to provide a continuous record of barrier disruption (Fig. 2).

Two experiments were carried out to observe the effects of the metabolic state on the electrical resistance. The effect of superfusing metabolic poisons, 1 mM-NaCN plus 1 mM-iodoacetic acid, was investigated, and resistance was measured when the superfusate was at room temperature. Resistance measurements were also made in rats which were dead.

Electron microscopy

Ionic lanthanum forms an electron dense precipitate with phosphate and hence is useful as an EM tracer for ion permeability at the blood–brain barrier (Bundgaard, 1982). Pial vessels at the surface of the cerebrum were exposed in 17- and 21-day gestation fetuses and in 1- and 10-day rats

($n = 3$ or 4 at each age), in the same way as described above for the electrophysiological measurements. The brain was initially superfused with phosphate-free Tris-buffered artificial CSF for 5–10 min, to wash out excess phosphates, followed with superfusion of 10 mM-$LaCl_3$ in the same CSF for up to 15 min, during which time the circulation was intact and vessels were well perfused. The brain was fixed *in situ* for 5 min with phosphate buffered fixative containing 2% paraformaldehyde and 2·5% gluteraldehyde, a procedure which caused La^{3+} to precipitate and blood flow to cease. The whole head was removed and immerse-fixed for a further 60 min after which the area of the cerebrum exposed to La^{3+} was excised and left in fixative overnight. After post-fixation in 1% phosphate-buffered osmium tetroxide, the tissues were dehydrated in graded alcohols, cleared in propylene oxide and embedded in epoxy resin (Emix). Ultrathin sections were stained with uranyl acetate and lead citrate and examined in the electron microscope (JEOL 100CX) for the distribution of lanthanum.

RESULTS

Transendothelial resistance during development

Electrical resistance of pial vessels was measured in fetal rats between 17 and 21 days gestation, in 1- to 10-day-old neonates, and in 28- to 33-day rats (Fig. 3). There was a significant change in resistance during development (analysis of variance, $P < 0{\cdot}001$), increasing acutely from a mean of 323 Ω cm² at 20 days gestation to 1128 Ω cm² at 21 days gestation. Resistance was constant in 17- to 20-day fetuses, and there was no further change after birth following the increase at 21 days gestation. The results were therefore divided into fetuses of 17–20 days gestation and rats from 21 days gestation and older; there was a significant difference (unpaired t test, $P < 0{\cdot}001$) between the means of the two groups, 310 ± 23 Ω cm² ($n = 78$ vessels, fourteen fetuses from eight mothers) and 1215 ± 110 Ω cm² ($n = 131$ vessels, twenty-seven animals). In 17- to 20-day fetuses, vessel resistance ranged from 30–1000 Ω cm², with 85% of vessels below 500 Ω cm² (Fig. 4). Resistance in rats of 21 days gestation and older varied from 30–5900 Ω cm², with 65% greater than 500 Ω cm² (Fig. 4).

Transendothelial resistance and vessel type

There was no significant difference in electrical resistance between arterial and venous vessels in fetal rats (Fig. 5). In postnatal rats, however, arterial vessels had a higher electrical resistance than venous vessels (significant at ages 8–10 and 28–33 days, unpaired t tests, $P < 0{\cdot}05$ and $P < 0{\cdot}01$, respectively). Taking rats of 21 days gestation and older as a group, resistance was significantly greater (unpaired t test, $P < 0{\cdot}01$) in arterial than venous vessels, with means of 1490 ± 170 Ω cm² ($n = 68$) and 918 ± 127 Ω cm² ($n = 63$), respectively. The variation observed in rats of 21 days gestation and older, therefore, was due in part to the difference between venous and arterial vessels (Fig. 6).

Transendothelial resistance with vessel diameter

There was no relation between electrical resistance and vessel diameter in 17- to 20-day fetuses (mean diameter of vessels from which measurements were made was 33 ± 1 μm, range 10–60 μm). Also, in rats from 21 days gestation and older, resistance did not change significantly with vessel diameter (analysis of variance, $P > 0{\cdot}1$; mean diameter 37 ± 1 μm, range 15–60 μm), when arterial and venous vessels were treated separately or combined (Fig. 7). There was, however, a tendency for

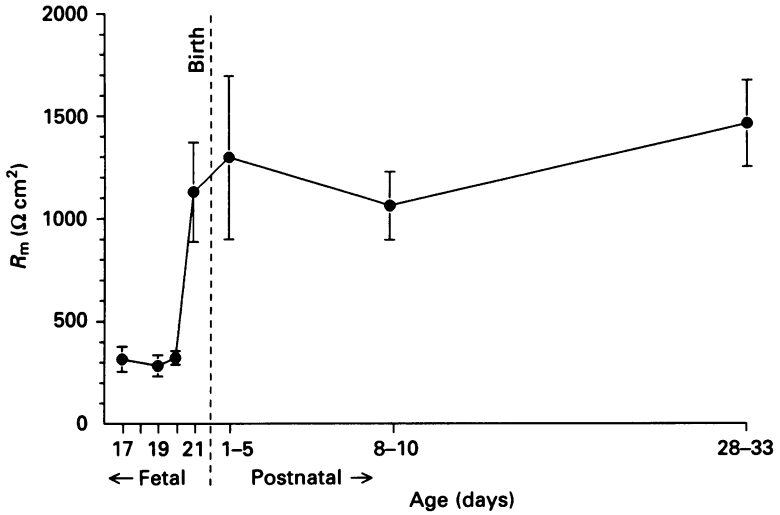

Fig. 3. Change in transendothelial resistance with age. Electrical resistance increased sharply at 21 days gestation, from $310 \pm 23\ \Omega\ cm^2$ in 17–20-day fetuses to $1215 \pm 110\ \Omega\ cm^2$ in 21-day fetuses and older rats. Points are means ± S.E.M., $n = 13$–52 vessels from at least three animals.

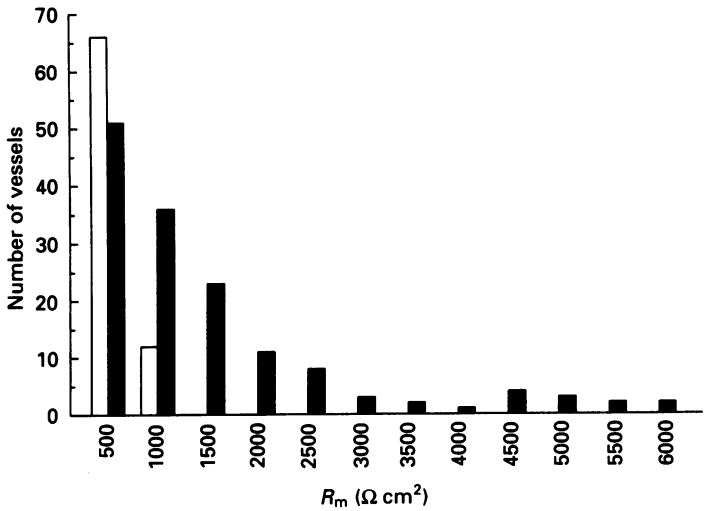

Fig. 4. Range of resistances in vessels from 17- to 20-day fetuses (open bars) and from 21-day fetuses and older rats (filled bars). In 17- to 20-day fetuses, most vessels were below $500\ \Omega\ cm^2$, while in 21-day fetuses and older rats, there was a wide distribution of resistances up to $6000\ \Omega\ cm^2$.

resistance to be lower in vessels > 50 μm, and this was particularly marked in arteries, where values obtained were close to those in veins.

Transendothelial resistance and length of exposure

The length of exposure is a measure of the experimental period with zero as the time at which the arachnoid mater was removed and the pial surface first uncovered. (The brain surface was superfused continuously with artificial CSF at 35 °C and at no

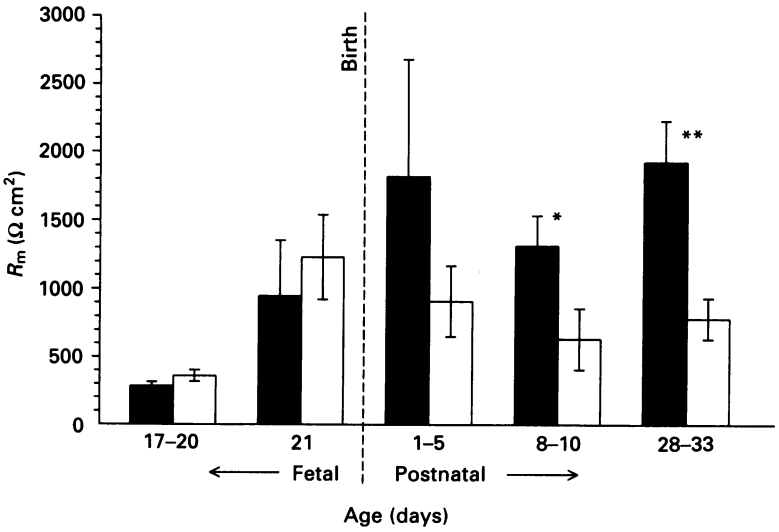

Fig. 5. Resistance in arterial (filled bars) and venous (open bars) blood vessels during development. Arterial vessels had a higher electrical resistance than venous vessels in postnatal rats. One and two asterisks represent a significant difference between vessel type (unrelated t test), where $P < 0{\cdot}05$ and $0{\cdot}01$, respectively.

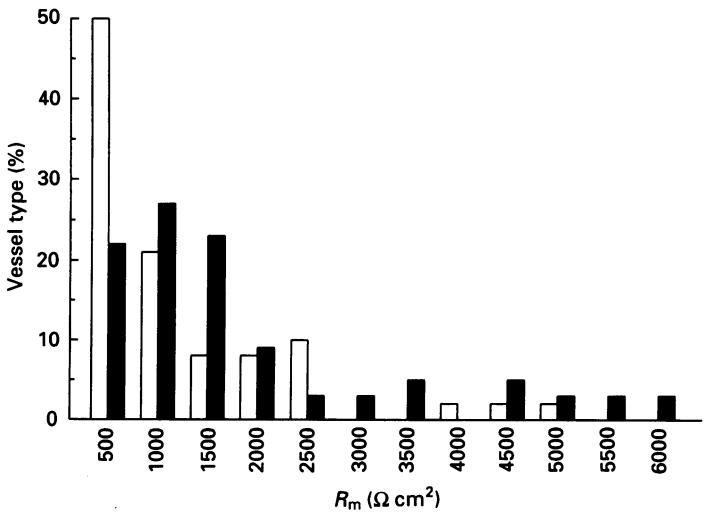

Fig. 6. Resistance in venous (open bars) and arterial (filled bars) vessels from 21-day fetuses and older rats. The venous supply had a larger proportion of low resistance vessels less than 500 Ω cm^2 compared with arterial vessels, where most vessels were in the range 500–1500 Ω cm^2.

time were pial vessels exposed to air.) In 17- to 20-day fetuses, resistances were low from the start (less than 10 min exposure) and did not change during the normal 30–60 min experimental period. In rats from 21 days gestation and older, there was no significant change in resistance during a 120 min period (analysis of variance, $P > 0{\cdot}1$), when arterial and venous vessels were treated separately or combined (Fig.

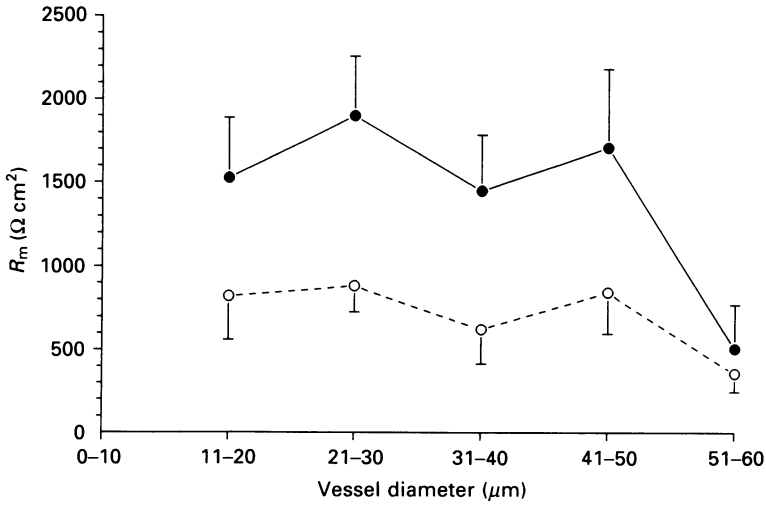

Fig. 7. Variation in resistance with vessel diameter in 21-day fetuses and older rats, in arterial (●) or venous (○) vessels. There was no significant overall change in resistance with diameter. However, resistance was lower in vessels larger than 50 μm diameter, particularly in arterial vessels.

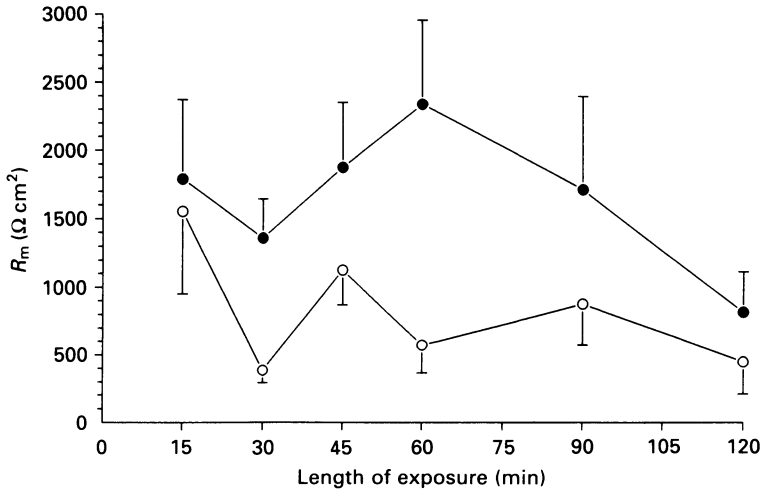

Fig. 8. Variation in resistance with length of exposure in 21-day fetuses and older rats, in arterial (●) and venous (○) vessels. Resistance did not change significantly with increasing length of exposure of the brain. After 90 min, however, resistance was lower, particularly in arterial vessels.

8). In arterioles over 90 min exposure, however, resistance was lower and similar to that in venules.

Blood–brain barrier disruption

In paired results from continuous recordings, resistance fell by an average of 68% ($n = 5$) during exposure to hyperosmotic CSF containing 250 mM-mannitol (Fig. 2). All results, including continuous recordings and measurements made on different

vessels, gave a mean resistance which was significantly lower in mannitol than in controls (unpaired t test, $P < 0{\cdot}05$), $203 \pm 38\ \Omega\ cm^2$ ($n = 24$) and $940 \pm 263\ \Omega\ cm^2$ ($n = 21$), respectively (Fig. 9). On return to normal CSF, resistance partially recovered to $456 \pm 87\ \Omega\ cm^2$ ($n = 21$), lower than but not significantly different from controls

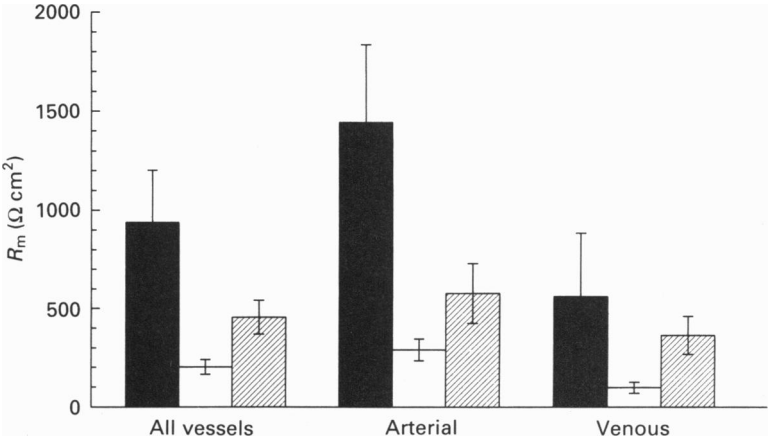

Fig. 9. Effect of osmotic shock on resistance. In all vessels combined (total of sixty-six vessels), the resistance in mannitol (open bars) was significantly lower than controls (closed bars), and resistance recovered partially to a level lower, but not significantly different from controls, and significantly higher than in mannitol (hatched bars). The proportional reduction in mannitol was similar in arterial and venous vessels, but the effect was to reduce venous resistance to a lower level than for arterial vessels.

(unpaired t test, $P > 0{\cdot}05$), and significantly greater than in mannitol (unpaired t test, $P < 0{\cdot}01$). The response was seen in both arterioles and venules. The percentage decrease in hyperosmolar solution was similar in both vessel types, but the resistance was significantly lower in hyperosmotic venules than arterioles (unpaired t test, $P < 0{\cdot}05$), 98 ± 28 and $291 \pm 56\ \Omega\ cm^2$ respectively (Fig. 9).

Addition of the metabolic poisons NaCN plus iodoacetic acid resulted in a rapid fall in resistance within 5 min, from a mean control resistance of 944 ± 213 ($n = 10$) to $102 \pm 12\ \Omega\ cm^2$ ($n = 3$), and with long exposure eventually fell to zero. Similarly, in rats which were dead there was no transendothelial electrical resistance. In rats where the superfusate was at room temperature (20 °C) resistance was also low, with a mean of $222 \pm 31\ \Omega\ cm^2$ ($n = 6$).

Electron microscopic studies

The arachnoid mater is the site of the meningeal barrier (Fig. 10*A*), and in young rats can be removed without damaging the underlying pial vessels (Fig. 10*B*). Pial vessels generally had a partial covering of pericytes, but the walls of smaller vessels used in this study did not have layers of smooth muscle and were devoid of the perivascular sheath of astrocytic end-feet, characteristic of parenchymal blood vessels. When the arachnoid was removed, lanthanum superfused over the brain had direct access to the pial vessel endothelium and was seen as dark deposits at the pial surface, within the brain extracellular space, and the endothelial basement membrane (Fig. 10*B*, *C*). In all ages studied, lanthanum was never observed within the vessel

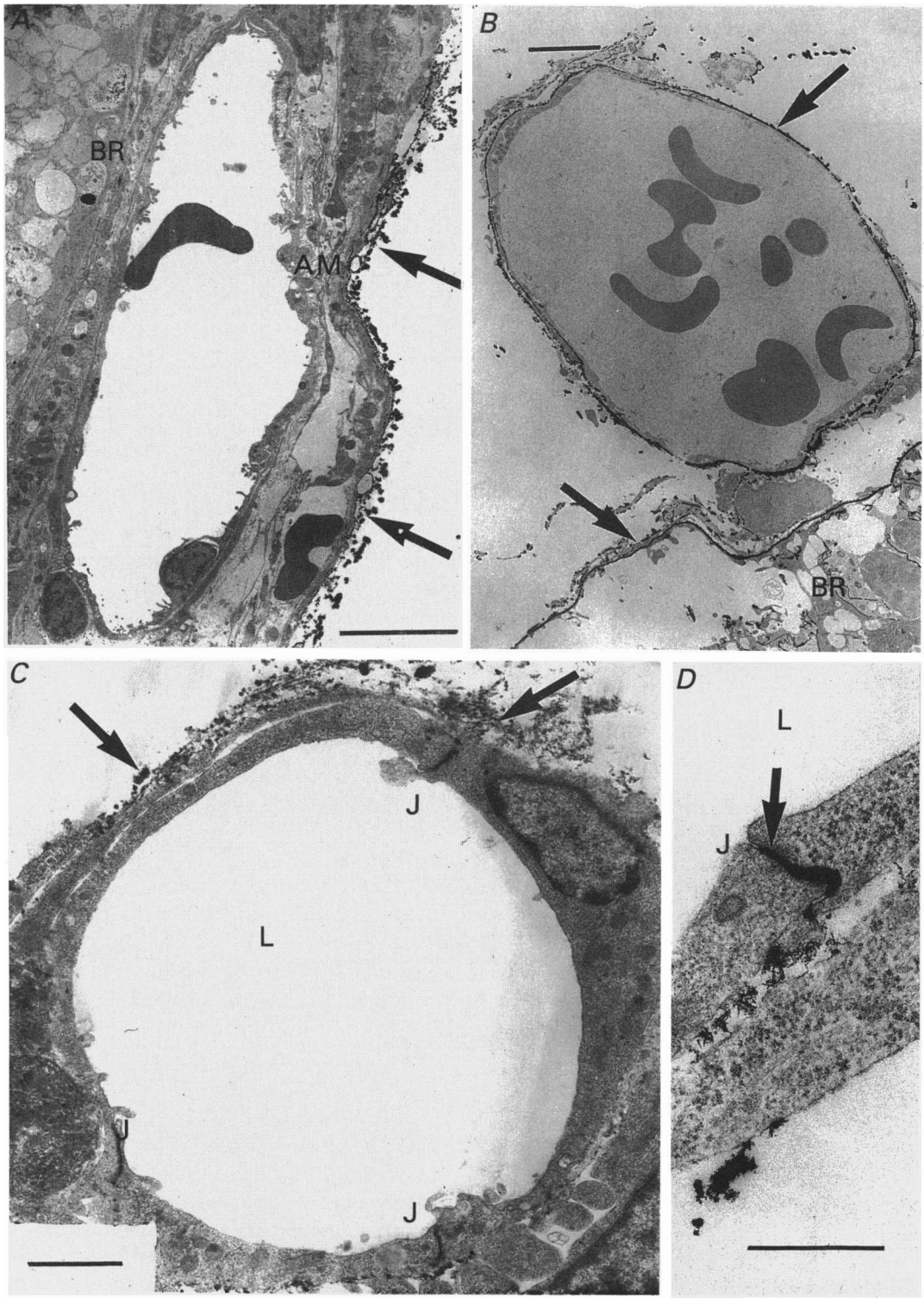

Fig. 10. For legend see facing page.

lumen at the endothelial apical membrane (vessels from 10-day neonate and 17-day fetus are illustrated in Fig. 10*B*, *C*) but was seen to accumulate within the interendothelial cleft in the region of the apical tight junctions (Fig. 10*D*).

DISCUSSION

Site of electrical resistance in pial vessels

Electrical resistance has been used to study ion permeability in many epithelia (Ussing & Windhager, 1964; Frömter & Diamond, 1972; Zeuthen & Wright, 1981; Crone & Christensen, 1981; Olesen & Crone, 1983; Rechthand & Rapoport, 1987; Hargittai, Butt & Lieberman, 1990), and in cerebral blood vessels (Crone & Olesen, 1982; Olesen, 1986; Butt, 1988; Olesen, 1989), and is a measure of both cellular and paracellular ion transport. The electrical resistance measured in the experiments described here is likely to represent the low but measurable ion permeability of endothelial intercellular junctions, since the membrane resistance of cerebral endothelium is likely to be very high, in the order of 10–25 kΩ cm^2 as in cultured aortic endothelial cells (Olesen, Davies & Clapham, 1988), and because the major route for passive ion transport across the blood–brain barrier in pial vessels appears to be paracellular (Crone, 1984). Furthermore, unlike parenchymal vessels, pial vessels are not enveloped with glial end-feet (Nabeshima, Reese, Landis & Brightman, 1975; Bundgaard, 1982) as shown in Fig. 10, and the cerebral endothelium can thus be studied directly. We have shown that in rats, pial vessels have a high electrical resistance typical for the blood–brain barrier, and that the high resistance developed at the time of birth, indicating a decrease in ion permeability. Parallel electron microscopic studies demonstrated that pial vessels in the rat are tight to ionic lanthanum, and that tight intercellular junctions were present at the blood–brain barrier as early as fetal day 17.

The fetal blood–brain barrier

Electrical resistance of pial vessels in 17- to 20-day fetuses was 300 Ω cm^2, lower than the 2000 Ω cm^2 typical for tight blood vessels (Crone & Olesen, 1982), but considerably higher than the 2 Ω cm^2 observed in leaky mesenteric blood vessels (Crone & Christensen, 1981), or the 20–30 Ω cm^2 as in muscle vessels (Olesen & Crone, 1983) and choroid plexus epithelium (Zeuthen & Wright, 1981). On the other hand, interendothelial cell junctions in pial vessels were impermeable to ionic lanthanum at this age (Fig. 10), as seen in the mature blood–brain barrier (Bouldin & Krigman, 1975; Bundgaard, 1982), whereas low-resistance epithelia such as the choroid plexus are leaky to lanthanum (Bouldin & Krigman, 1975). The fetal blood–brain barrier in rats, therefore, has ion permeability properties intermediate between tight and leaky

Fig. 10. Tightness of pial vessels to ionic lanthanum in 10-day postnatal rats (*A* and *B*) and in 17-day gestation fetuses (*C* and *D*). In *A*, lanthanum (arrows) superfused over the cortex is stopped from reaching the brain surface (BR) by the arachnoid mater (AM), but in (*B*) and (*C*) the arachnoid has been removed and lanthanum (arrows) has immediate and direct access to the brain and to surface blood vessels. Lanthanum (arrows) was not observed within the vessel lumen (L) in fetal or postnatal rats, but was stopped by tight intercellular junctions (J) and accumulated within the intercellular clefts, as shown at higher magnification in *D*. Scale bars: *A* and *B*, 5 μm; *C*, 1 μm; *D*, 0·5 μm.

epithelia (Frömter & Diamond, 1972), similar to the perineurium in crayfish (Hargittai *et al.* 1990) and frog (Rechthand & Rapoport, 1987), which have relatively low resistances of 250 and 478 Ω cm^2, respectively, but are also impermeable to lanthanum. The results indicate that tight junctions are present during early development in the rat, which is consistent with previous studies using fluorescein-labelled albumin (Olsson, Klatzo, Sourander & Steinwall, 1968).

Change in electrical resistance during development

There was an acute increase in resistance to 1200 Ω cm^2 in 21-day fetuses, and there was no further increase in resistance after birth (Fig. 3). In previous experiments, ion regulation of the brain interstitial fluid was seen after birth but not in 21-day fetuses (Jones & Keep, 1987, 1988). Twenty-one days is the normal gestation period in rats, but gestational age and proximity of birth are difficult to measure accurately, and can only be defined within a ± 12 h margin. The difference between the two studies probably reflects this, and we conclude therefore that both the increase in electrical resistance and the onset of brain interstitial ion regulation occur immediately prior to birth over a relatively short period of time.

The mature blood–brain barrier

The mean electrical resistance across the walls of blood vessels on the pial surface of the brain in 28- to 33-day-old rats was about 1500 Ω cm^2 (Fig. 3). This is within the range seen in corresponding studies on brain surface vessels in dogfish (Butt, 1988) and in frog (Crone & Olesen, 1982), which were 1200 and 1900 Ω cm^2, respectively, and is also typical of those for tight epithelia such as the frog skin (Ussing & Windhager, 1964). Rats of this age are post-weaning but prepubescent, and the regulatory and transport mechanisms at the blood–brain and blood–CSF barriers appear to be fully developed (Betz & Goldstein, 1981; Møllgård & Saunders, 1986; Jones & Keep, 1987, 1988; Johanson, 1989). Older rats were not used because removing the arachnoid mater to expose the pial vessels without causing damage is difficult. Furthermore, drilling of the skull is thought to disrupt the blood–brain barrier (Olesen, 1987), and drilling could be minimized or avoided in the young rats used here. Smith & Rapoport (1986) calculated an electrical resistance of 8000 Ω cm^2 for brain parenchymal vessels from the combined permeability of radioisotopic sodium, potassium and chloride in the adult rat. This higher value may reflect a difference in the measuring technique or a difference between pial and parenchymal vessels. It should be noted, however, that some values of 6000 Ω cm^2 were obtained in these experiments and that any potential deterioration of the preparation would tend to lower the measured values, so it is conceivable that the higher figures reflect the true resistance of the blood–brain barrier.

Comparison of arterial and venous vessels

Arterioles had a significantly higher resistance than venules in postnatal rats; for example, in the oldest age group mean resistances were 1924 and 781 Ω cm^2, respectively (Fig. 5). Two possible explanations for this are that there may be differences in tight junction structure between the two vessel types, or that venous vessels are more susceptible to damage. Freeze-fracture studies have shown that arterioles, capillaries and venules have intercellular junctions of similar strand

number and organization, whereas collecting veins have few, discontinuous strands and are therefore potentially leaky (Nagy, Peters & Hüttner, 1984). This is not inconsistent with the finding that resistance was low (300 Ω cm^2) in larger venules, with a diameter 51–60 μm (Fig. 7), but does not explain the difference between the smaller vessels. In one study (Olesen, 1987), pial venules but not arterioles developed focal leaks to large MW solutes such as albumin (MW 69 kDa), soon after removal of the skull. On the other hand, Mayhan & Heistad (1985) found that normally no vessels were leaky to a series of Dextrans, but that experimentally induced disruption occurred first in small venules (15–30 μm) and later in arterioles. In this study, the mean resistance in venous vessels was 918 Ω cm^2, reflecting a tight barrier, although further analysis showed that 19% of venules had values $\leqslant 200\ \Omega$ cm^2, suggesting that individual vessels may be damaged. Only 2% of arterioles had resistances this low, indicating that barrier disruption is greater in venous vessels. A more obvious deterioration in the preparation was the low resistance in both vessel types with exposure times over 90 min (Fig. 8).

Blood–brain barrier disruption

Hyperosmotic shock, metabolic poisoning and low temperatures all caused a fall in resistance in postnatal rats, but only to 100–300 Ω cm^2. This suggests that normal metabolic functioning of endothelial cells is required to maintain full integrity of the tight junctions, as found in frog pial vessels (Olesen, 1986).

It is well established that hyperosmotic shock leads to a disruption of the blood–brain barrier, probably by modification of the tight junctions (Brightman, Hori, Rapoport, Reese & Westergaard, 1973; Robinson & Rapoport, 1987). The total osmolarity of 530 mosM used here, is above the threshold for osmotic disruption of the rat barrier which in a radioisotope study resulted in a 3-fold increase in ion permeability (Cserr, DePasquale & Patlak, 1987). In this study, electrical resistance decreased in both arterioles and venules during hyperosmotic shock (Fig. 9), suggesting both vessel types had increased ion permeability. Hyperosmotic disruption in surface vessels has been observed previously only in venules (Rapoport, Hori & Klatzo, 1972; Mayhan & Heistad, 1985), but this was using large MW (4–79 kDa) tracers, and changes in ion permeability would not have been detected. In another study, on parenchymal vessels, capillaries and arterioles were the major sites for barrier disruption during hyperosmotic shock (Brightman *et al.* 1973). It is possible, that the lower mean resistance of 100 Ω cm^2 in venules during hyperosmotic shock, which is similar to that of leaky epithelia (Frömter & Diamond, 1972), indicates a level at which the barrier is permeable to both ions and to large MW solutes. Conversely, a mean resistance of 300 Ω cm^2, as seen in hyperosmotic arterial vessels, is similar to the 'intermediate' fetal blood–brain barrier and to other epithelia (Frömter & Diamond, 1972; Rechthand & Rapoport, 1987; Hargittai *et al.* 1990) and may indicate a barrier which is permeable to ions but not to large solutes.

Electrical resistance and ion regulation

Ion regulation of the brain interstitial fluid is dependent on the activity of glial cells, ion transport at the cerebral endothelium, and the low paracellular permeability of the blood–brain barrier. The mature blood–brain barrier is tight to ionic lanthanum, has a high resistance, and is capable of a high degree of ion homeostasis.

In fetal rats, interendothelial junctions are tight to lanthanum, but have a low resistance, and brain interstitial fluid ion regulation is not developed. We suggest that a decrease in permeability of the blood–brain barrier as reflected in an increase in electrical resistance immediately prior to birth is the most likely explanation for the onset of brain interstitial fluid ion homeostasis in rats, for the following reasons. Firstly, glial cells are unlikely to be responsible since they do not mature until the second postnatal week and later (Caley & Maxwell, 1970). This is supported by experiments in the rat optic nerve where glial regulatory mechanisms do not develop until 2–3 weeks after birth (Ransom, Carlini & Connors, 1986). Secondly, ion transport mechanisms at the blood–brain barrier appear to change postnatally in a gradual manner rather than increase acutely at birth (Betz & Goldstein, 1981; Johanson, 1989). Furthermore, the high mitochondrial content of brain capillary endothelium which is thought to be related to high levels of transport activity (Oldendorf, Cornford & Brown, 1977), is present at the same level in fetal and adult brain capillaries (Keep, R. F. & Jones, H. C., unpublished observation). Some ion transport mechanisms are probably present during early development of the blood–brain barrier since fetal rats maintain a gradient for K^+ between plasma and insterstitial fluid under normal conditions (Jones & Keep, 1987). Finally, the onset of brain interstitial fluid regulation affects both K^+ and Ca^{2+} equally (Jones & Keep, 1987, 1988), which is consistent with a non-selective change in permeability at the blood–brain barrier rather than a change in ion-specific transport mechanisms.

The mean resistance of vessels in 17- to 20-day fetuses was 300 Ω cm^2 and indicates an intermediate barrier, with ion permeability properties which fall between those of leaky and tight epithelia, as discussed above. A similar mean resistance was seen during hyperosmotic shock (Fig. 9) and indicates a barrier which is leaky to ions (Cserr *et al.* 1987). In fetuses this would limit the ability of the blood–brain barrier to maintain interstitial fluid independent of plasma (Jones & Keep, 1987, 1988). If, however, only a small fraction of the paracellular pathway is accessible for ion movement (Crone, 1984), and if leaky sites are focal (Mayhan & Heistad, 1985; Olesen, 1987) and occur infrequently, the probability of observing one in electron microscopic studies would be remote, thus explaining the observed impermeability of the fetal barrier to lanthanum. However, a low resistance alone does not necessarily indicate an inability to regulate ions, and other intermediate epithelia, such as the crayfish perineurium (Hargittai *et al.* 1990), and even a leaky epithelium such as the choroid plexus which has a resistance of only 20 Ω cm^2 (Zeuthen & Wright, 1981), are capable of a degree of ion homeostasis more typical of tight epithelia, due to very active cellular transport processes. Cellular transport of ions at the blood–brain barrier may be important for interstitial ion regulation (Betz & Goldstein, 1981; Abbott *et al.* 1986), but to be most effective there must be a low paracellular shunt.

Supported by the Wellcome Trust and MRC. We thank Mr J. Pacy for assistance with electron microscopy.

REFERENCES

ABBOTT, N. J., BUTT, A. M. & WALLIS, W. (1986). The Na–K ATPase of the blood–brain barrier: a microelectrode study. *Annals of the New York Academy of Sciences* **481**, 390–391.

BETZ, A. L. & GOLDSTEIN, G. W. (1981). Developmental changes in metabolism and transport properties of capillaries isolated from rat brain. *Journal of Physiology* **312**, 365–376.

BOULDIN, T. W. & KRIGMAN, M. R. (1975). Differential permeability of cerebral capillary and choroid plexus to lanthanum ions. *Brain Research* **99**, 444–448.

BRADBURY, M. W. B. (1979). *The Concept of a Blood–Brain Barrier*. Wiley, Chichester.

BRIGHTMAN, M. W., HORI, M., RAPOPORT, S. I., REESE, T. S. & WESTERGAARD, E. (1973). Osmotic opening of tight junctions in cerebral epithelum. *Journal of Comparative Neurology* **152**, 317–326.

BRIGHTMAN, M. W. & REESE, T. S. (1969). Junctions between intimately apposed cell membranes in the vertebrate brain. *Journal of Cell Biology* **40**, 648–677.

BUNDGAARD, M. (1982). Ultrastructure of frog cerebral and pial microvessels and their impermeability to lanthanum ions. *Brain Research* **241**, 57–65.

BUTT, A. M. (1988). Electrical resistance of cerebral blood vessels in the skate and dogfish. *Journal of Physiology* **399**, 29*P*.

BUTT, A. M. & JONES, H. C. (1990). Electrical resistance across the developing blood–brain barrier in anaesthetized rats. *Journal of Physiology* **423**, 32*P*.

CALEY, D. W. & MAXWELL, D. S. (1970). Development of the blood vessels and extracellular spaces during postnatal maturation of rat cerebral cortex. *Journal of Comparative Neurology* **138**, 31–48.

CRONE, C. (1984). Lack of selectivity to small ions in paracellular pathways in cerebral and muscle capillaries of the frog. *Journal of Physiology* **353**, 317–337.

CRONE, C. & CHRISTENSEN, O. (1981). Electrical resistance of a capillary endothelium. *Journal of General Physiology* **77**, 349–371.

CRONE, C. & OLESEN, S.-P. (1982). Electrical resistance of brain microvascular endothelium. *Brain Research* **241**, 49–55.

CSERR, H. F., DEPASQUALE, M. & PATLAK, C. S. (1987). Volume regulatory influx of electrolytes from plasma to brain during acute hyperosmolality. *American Journal of Physiology* **253**, F530–537.

FRÖMTER, E. & DIAMOND, J. (1972). Route for passive ion permeation in epithelia. *Nature* **235**, 9–13.

HARGITTAI, P. T., BUTT, A. M. & LIEBERMAN, E. M. (1990). High potassium selective permeability and extracellular ion regulation in the glial perineurium (blood–brain barrier) of the crayfish. *Journal of Neuroscience* (in the Press).

HODGKIN, A. L. (1951). The ionic basis of electrical activity in nerve and muscle. *Biological Reviews* **26**, 339–409.

JOHANSON, C. E. (1989). Ontogeny and phylogeny of the blood–brain barrier. In *Implications of the Blood–Brain Barrier and its Manipulation*, vol. 1, ed. NEUWELT, E., pp. 157–198. Plenum, New York.

JONES, H. C. & KEEP, R. F. (1987). The control of potassium concentration in the cerebrospinal fluid and brain interstitial fluid of developing rats. *Journal of Physiology* **383**, 441–453.

JONES, H. C. & KEEP, R. F. (1988). Brain fluid calcium concentration and response to acute hypercalcaemia during development in the rat. *Journal of Physiology* **402**, 579–593.

KATZ, B. (1966). *Nerve, Muscle and Synapse*, pp. 73–75. McGraw-Hill, New York.

MAYHAN, W. G. & HEISTAD, D. D. (1985). Permeability of blood–brain barrier to various sized molecules. *American Journal of Physiology* **248**, H712–718.

MØLLGÅRD, K. & SAUNDERS, N. R. (1986). The development of the human blood–brain and blood–CSF barriers. *Neuropathology and Applied Neurobiology* **12**, 337–358.

NABESHIMA, S., REESE, T. S., LANDIS, D. M. D. & BRIGHTMAN, M. W. (1975). Junctions in the meninges and marginal glia. *Journal of Comparative Neurology* **164**, 127–170.

NAGY, Z., PETERS, H. & HÜTTNER, I. (1984). Fracture faces of cell junctions in cerebral endothelium during normal and hyperosmotic conditions. *Laboratory Investigation* **50**, 313–322.

OLDENDORF, W. H., CORNFORD, M. E. & BROWN, W. J. (1977). The large apparent work capability of the blood–brain barrier: a study of the mitochondrial content of capillary endothelial cells in brain and other tissues of the rat. *Annals of Neurology* **1**, 409–417.

OLESEN, S.-P. (1986). Rapid increase in blood–brain barrier permeability during severe hypoxia and metabolic inhibition. *Brain Research* **368**, 24–29.

OLESEN, S.-P. (1987). Leakiness of rat brain microvessels to fluorescent probes following craniotomy. *Acta physiologica scandinavica* **130**, 63–68.

OLESEN, S.-P. (1989). An electrophysiological study of microvascular permeability and its modulation by chemical mediators. *Acta physiologica scandinavica* **136**, suppl. 579.

OLESEN, S.-P. & CRONE, C. (1983). Electrical resistance of muscle capillary endothelium. *Biophysical Journal* **42**, 31–41.

OLESEN, S.-P., DAVIES, P. F. & CLAPHAM, D. E. (1988). Muscarinic acetylcholine-activated K^+ current in bovine aortic endothelial cells. *Circulation Research* **62**, 1059–1064.

OLSSON, Y., KLATZO, I., SOURANDER, P. & STEINWALL, O. (1968). Blood–brain barrier to albumin in embryonic, newborn and adult rats. *Acta neuropathologica* **10**, 117–122.

RANSOM, B. R., CARLINI, W. G. & CONNORS, B. W. (1986). Brain extracellular space: developmental studies in rat optic nerve. *Annals of the New York Academy of Sciences* **481**, 87–104.

RAPOPORT, S. I., HORI, M. & KLATZO, I. (1972). Testing of the hypothesis for osmotic opening of the blood–brain barrier. *American Journal of Physiology* **223**, 323–331.

RECHTHAND, E. & RAPOPORT, S. I. (1987). Regulation of the microenvironment of peripheral nerve: role of the blood–nerve barrier. *Progress in Neurobiology* **28**, 303–343.

ROBINSON, P. J. & RAPOPORT, S. I. (1987). Size selectivity of blood–brain barrier permeability at various times after osmotic opening. *American Journal of Physiology* **253**, R459–466.

SMITH, Q. R. & RAPOPORT, S. I. (1986). Cerebrovascular permeability coefficients to sodium, potassium and chloride. *Journal of Neurochemistry* **46**, 1732–1742.

USSING, H. H. & WINDHAGER, E. E. (1964). Nature of the shunt path and active sodium transport path through frog skin epithelium. *Acta physiologica scandinavica* **61**, 484–504.

ZEUTHEN, T. & WRIGHT, E. M. (1981). Epithelial potassium transport: tracer and electrophysiological studies in choroid plexus. *Journal of Membrane Biology* **60**, 105–128.